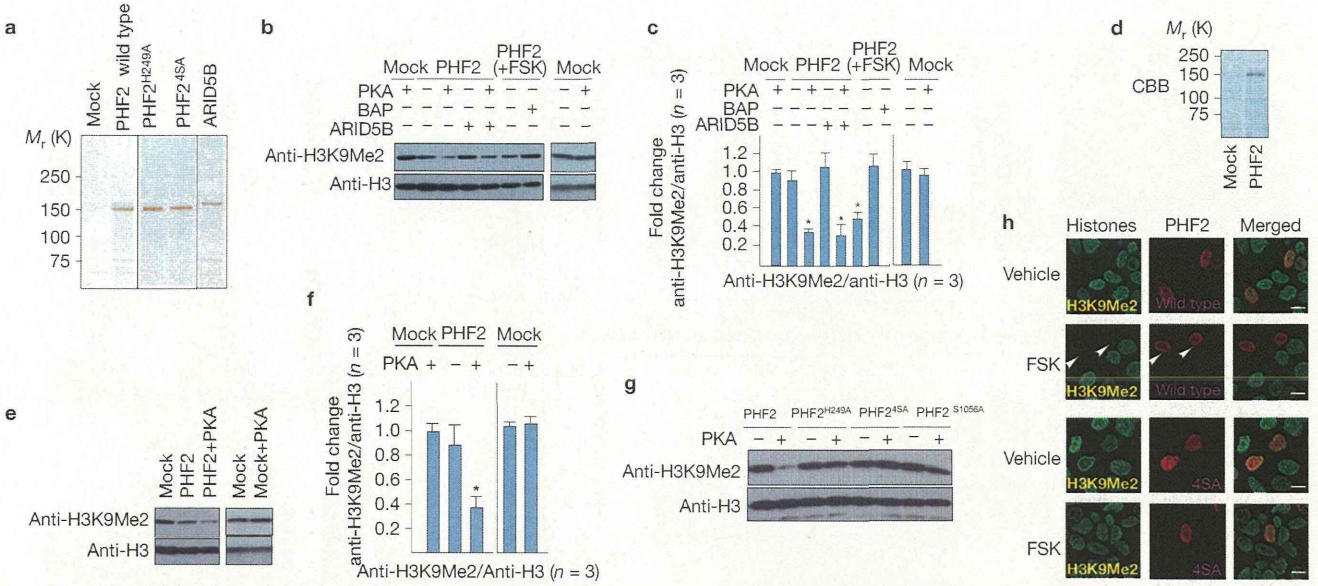

Figure 3 PKA-dependent demethylase activity of the PHF2–ARID5B complex. (**a**) The indicated proteins were purified to near homogeneity from 293F cells. Purification of PHF2 mutants is shown in Supplementary Fig. S5e. Note that purified PHF2 did not include ARID5B (Supplementary Fig. S5f). (**b**,**c**) *In vitro* histone demethylation assay. Purified PHF2 protein or PHF2 mutants were incubated with either PKA or BAP as indicated, and *in vitro* demethylation assays were carried out with/without purified ARID5B protein. (**c**) The signal intensity of three independent experiments (performed as in **b** and Supplementary Fig. S8d) was quantified. Data are averages ± s.d. The asterisks show $P < 0.05$ in Student's *t*-test. (**d**–**f**) Recombinant PHF2 protein purified to near homogeneity from Sf9 cells was phosphorylated by PKA, and *in vitro* demethylation assay was carried out as in **b**,**c**. (**f**) Data are averages ± s.d. ($n = 3$, Supplementary Fig. S8e). The asterisk shows $P < 0.05$ in Student's *t*-test. (**g**) *In vitro* histone demethylation assay as in **b** with the indicated PHF2 mutants. (**h**) H3K9Me2 demethylation activity of PHF2–ARID5B is FSK dependent *in vivo*. 293F cells transfected with wild-type or $PHF2^{4SA}$ were treated with FSK for 6 h. Scale bars, 40 μm. Uncropped images of blots are shown in Supplementary Fig. S9.

homeostasis through induction of gluconeogenic enzymes, such as Pepck and G6Pase (refs 20–23). Chromatin immunoprecipitation (ChIP) analysis revealed glucagon–PKA-induced promoter binding of PHF2–ARID5B at the promoters of *Pepck* and *G6Pase* (Fig. 4a). Sequential ChIP (Re-ChIP) suggested that the endogenous PHF2–ARID5B complex associates with the *Pepck* promoter (Fig. 4b), without protein synthesis (Fig. 4b and Supplementary Fig. S6a). H89 abrogated glucagon-mediated recruitment of these factors (Supplementary Fig. S6b). PHF2 and ARID5B were co-recruited to *Pepck* promoter on similar time-courses (Supplementary Fig. S6c). Demethylation of H3K9Me2 was induced by FSK, coupled with PHF2 recruitment (Fig. 4a and Supplementary Fig. S6c). However, the H3K9Me1 level was not significantly altered by FSK treatment (Fig. 4a), suggesting that newly produced H3K9Me1 was sequentially demethylated by other H3K9 demethylase(s). H3K9Me3 signal was low in both the presence and absence of FSK (Fig. 4a), consistent with the notion that *Pepck* and *G6Pase* gene promoters are converted to euchromatin in hepatocytes.

We further explored the mechanism for PKA-dependent promoter recruitment of PHF2–ARID5B. Although ARID5B was dispensable for PHF2 enzymatic activity *in vitro* (Fig. 3b), ARID5B was required for promoter targeting of PHF2 and H3K9Me2 demethylation *in vivo* (Fig. 4c, lanes 9–12, 4d). Knockdown of PHF2 by RNA interference attenuated FSK-induced recruitment of ARID5B to the promoters (Fig. 4c, lanes 3–4, 4d), indicating the signal-sensing role of PHF2 in directing the complex to target promoters. A specific PHF2 mutant (H249A), lacking a conserved histidine essential for its lysine demethylation activity (Fig. 1g), was unable to anchor PHF2–ARID5B on the target gene promoter (Fig. 4c, lanes 7, 8). We reasoned that a lysine demethylation event occurred before chromatin association. Therefore, we determined whether ARID5B was a substrate for the PHF2 demethylase. Exogenously expressed ARID5B was lysine-methylated in hepatocytes in the absence of FSK (Fig. 5a, lane 2). PHF2 induced demethylation of ARID5B in the presence of FSK through the jmjC domain (Fig. 5a, lanes 3–4). ARID5B, but not other ARID family proteins, harbours a lysine motif (Lys 336) in the ARID domain that resembles the alignment around histone H3K9 (Supplementary Fig. S6d). When Lys 336 of ARID5B was replaced by alanine (K336A), the methylated form of ARID5B was no longer detected (Fig. 5a, lane 5). An anti-ARID5B-K336Me2 antibody was raised, and the specificity was confirmed by an enzyme-linked immunosorbent assay with methylated ARID5B (Supplementary Fig. S6e) as well as with unmethylated K336A or K336R mutants (Fig. 5b). We found that PHF2 promoted demethylation of ARID5B at Lys 336 (Fig. 5c). Catalytically inactive $PHF2^{H249A}$ increased the ARID5B K336Me2 mark (Fig. 5c), and endogenous ARID5B was demethylated following FSK treatment (Fig. 5d). Moreover, purified PHF2 protein demethylated ARID5B at Lys 336 *in vitro* (Fig. 5e). We then used a DNA pulldown (ABCD) assay to determine if demethylation of Lys 336-methylated ARID5B converted it to an active form on DNA binding. Only when cells were treated with FSK, ARID5B–PHF2 complex was recruited to synthetic oligonucleotides containing the *Pepck* promoter sequences[24,25] (Fig. 5f). FSK-dependent DNA binding of PHF2–ARID5B was abolished in $PHF2^{H249A}$ and $ARID5B^{K336A}$ mutants (Fig. 5f). Neither $PHF2^{H249A}$ nor $ARID5B^{K336A}$ supported FSK-mediated promoter recruitment and subsequent H3K9Me2 demethylation (Fig. 4c).

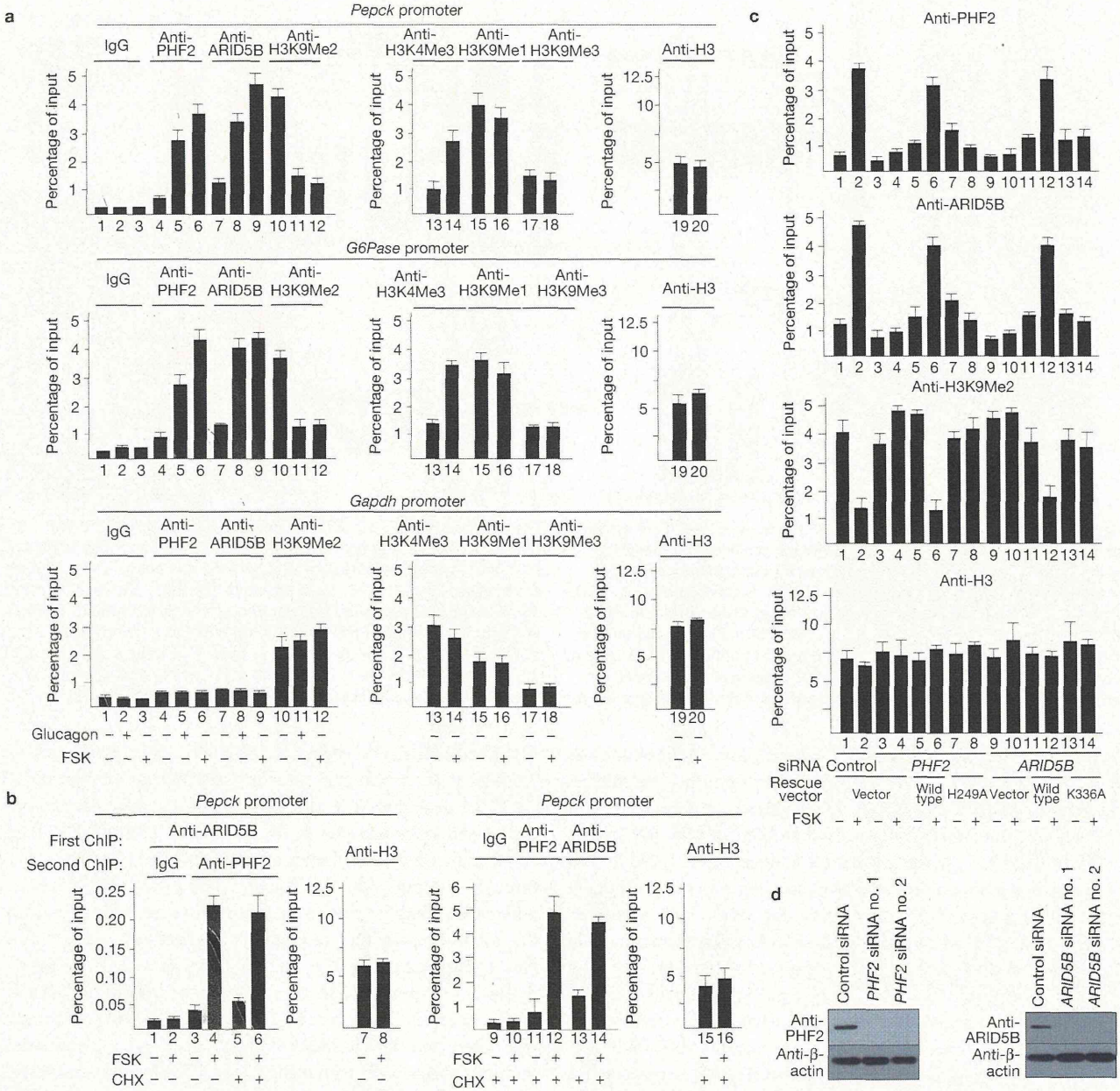

Figure 4 PKA-dependent promoter targeting of PHF2–ARID5B. (**a**) Endogenous PHF2–ARID5B complex is recruited to the promoter regions of *Pepck* and *G6Pase*, but not to that of *Gapdh*, in a glucagon–PKA-dependent manner. Hepatocytes were treated with the indicated compounds for 4 h, and ChIP assays were carried out using indicated antibodies. Data are average ± s.d. ($n = 3$). (**b**) ChIP and Re-ChIP assays. Hepatocytes were treated with the indicated compounds for 4 h, then sequentially immunoprecipitated with the indicated antibodies. Data are average ± s.d. ($n = 3$). (**c**) Promoter targeting and H3K9Me2 demethylase activities of PHF2–ARID5B mutants in ChIP assays. Hepatocytes were transfected with the indicated siRNAs for 24 h, then with the indicated rescue vector for a further 12 h. Then, cells were treated with FSK for 4 h and ChIP assays were carried out. Data are average ± s.d. ($n = 3$). (**d**) The knockdown efficiencies of siRNAs in immortalized hepatocytes were determined using samples in **c**. Uncropped images of blots are shown in Supplementary Fig. S9.

PHF2–ARID5B acts as a co-activator for HNF4α in liver of fasted mice

The transcriptional effects mediated by PHF2–ARID5B were assessed by monitoring gene expression in hepatocytes. PKA-dependent gene induction of *Pepck* and *G6Pase* was impaired (Fig. 6a) following knockdown of PHF2 or ARID5B in hepatocytes (Fig. 4d). The unphosphorylated PHF2 mutant ($PHF2^{4SA}$) was unable to confer the FSK response (Fig. 6a). As HNF4α is activated by the glucagon–PKA signalling pathway and serves as the primary transcriptional activator on *Pepck* and *G6Pase* promoters[21,22,26–28], we further characterized the transcriptional co-activation function of PHF2–ARID5B towards HNF4α. In a luciferase reporter assay in the presence of FSK (refs 12,29), PHF2 acted as a co-activator for HNF4α (Fig. 6b) as well as FXR (Supplementary Fig. S7) in 293F

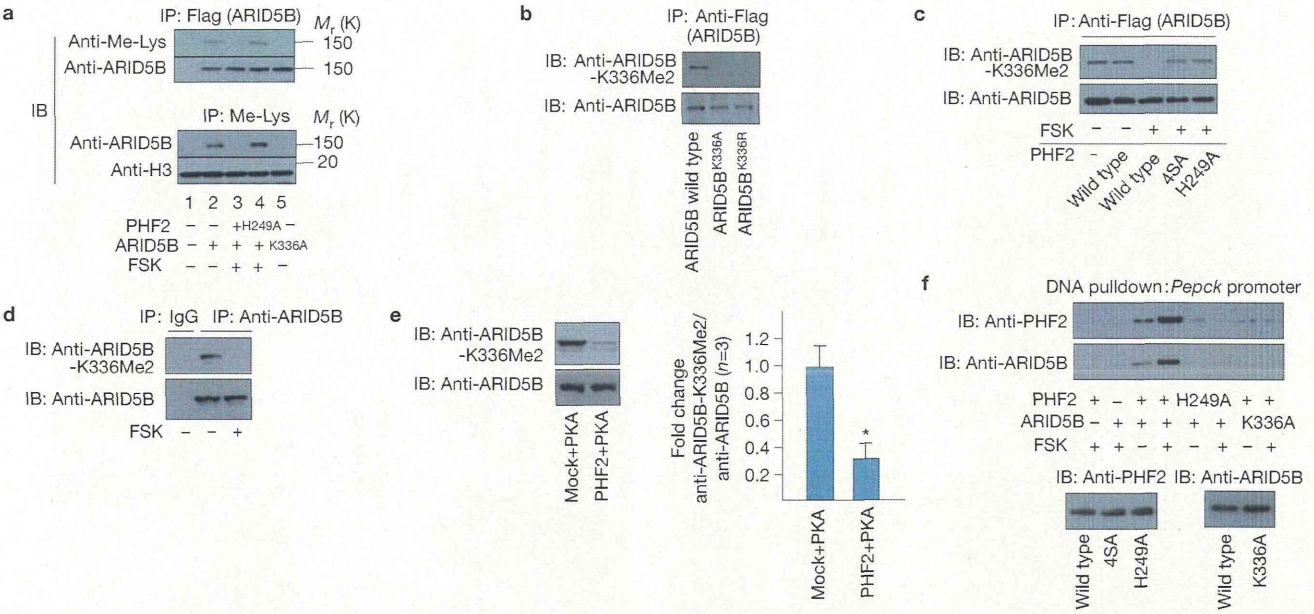

Figure 5 ARID5B directs PKA-dependent promoter targeting of PHF2. (**a**) PHF2 induces demethylation of ARID5B. The methylation state of ARID5B in 293F cells was examined using anti-ARID5B and anti-methyl-lysine antibodies. Wild-type, but not K336A, ARID5B is a lysine-methylated protein. (**b**) Confirmation of specificity of anti-ARID5B-K336Me2 antibody. 293F cells were transfected with the indicated ARID5B mutants and immunoprecipitated/blotted with the indicated antibodies. (**c**) Demethylation of ARID5B is dependent on the catalytic activity of PHF2 in hepatocytes as revealed by the specified anti-ARID5B-K336Me2 antibody. (**d**) Lys 336 methylation of endogenous ARID5B. 293F cells were treated with FSK for 4 h, then immunoprecipitation was carried out as indicated. (**e**) *In vitro* ARID5B demethylation assay. Flag–ARID5B purified from 293F cells was incubated with purified PHF2 (Fig. 3a), and the demethylation was detected by western blotting. The signal intensity of three independent experiments (in the upper panel and in Supplementary Fig. S8f) was quantified. Data are averages ± s.d. ($n = 3$). The asterisk shows $P < 0.05$ in Student's *t*-test. (**f**) DNA pulldown assay. The demethylase activity of PHF2 and the ARID domain of ARID5B are required for promoter DNA binding of PHF2–ARID5B in 293F cells. Cell lysates were mixed with avidin beads which were bound to biotin-conjugated oligonucleotides bearing the indicated promoter sequence. The bound protein was detected by western blotting. There were similar levels of expression of PHF2–ARID5B and their derivatives (lower panels). Uncropped images of blots are shown in Supplementary Fig. S9.

cells[24,25]. HNF4α was enriched with PHF2–ARID5B on the promoter of *Pepck* (Fig. 6c). Knockdown of HNF4α decreased recruitment of PHF2–ARID5B to the promoters (Fig. 6c) and loss of PKA-dependent gene induction (Fig. 6d). Thus, HNF4α and FXR have emerged as transcriptional activators co-activated by PHF2–ARID5B in glucagon–PKA-induced gene expression.

Finally, the physiological relevance of the proposed PHF2–ARID5B promoter targeting was examined under fasting conditions where PKA signal was activated by glucagon in intact animals. In fasted mice, co-recruitment of PHF2 with ARID5B was detected in the promoter regions of *Pepck* and *G6Pase* in liver (Fig. 6e) with the expected decrease in H3K9Me2 modification (Fig. 6e).

DISCUSSION

Here, we have identified a PKA-dependent histone demethylase complex that conferred signal-dependent activation of its responsive genes. Assembly of the PHF2–ARID5B complex, its recruitment to target promoters, and its H3H9Me2 demethylase activity were dependent on PKA activity. Thus, the PHF2–ARID5B complex seems to serve as a signal-sensing epigenetic determinant through removal of a repressive histone methylation mark[1,2,30,31] on the transcriptionally responsive promoters. The molecular basis of signal sensing by the PHF2–ARID5B complex is attributable to PKA-phosphorylation-dependent induction of PHF2 enzymatic activity and complex assembly with the DNA-binding subunit (ARID5B). Unlike PHF2, several other jmjC demethylases possess both jmjC and ARID domains within a single molecule[3,5,8,9]. Thus, segregation of these two key domains into separate subunits may enable PHF2 enzymatic activity to be linked to PKA signalling through assembly of the PHF2–ARID5B complex and intracomplex communication. Similarly, other jmjC demethylases that are inactive as single subunits may be functionally regulated through post-translational modifications and assembly with their complex partner components. The characterization of a signal-dependent histone demethylase provides further understanding of the regulatory mechanism for dynamic epigenetic modification in physiological contexts such as energy metabolism and homeostasis. □

METHODS

Methods and any associated references are available in the online version of the paper at http://www.nature.com/naturecellbiology

Note: Supplementary Information is available on the Nature Cell Biology website

ACKNOWLEDGEMENTS

We thank D. D. Moore for critical discussion, R. Sato and J. Inoue for providing materials, N. Moriyama and S. Fujiyama for technical assistance and M. Yamaki for manuscript preparation. This work was supported in part by Priority Areas from the Ministry of Education, Culture, Sports, Science and Technology, MEXT, Japan, JSPS, and The Naito Foundation (to F.O. and S.K.).

AUTHOR CONTRIBUTIONS

A.B., F.O. and S.K. designed the study. A.B., F.O., Y.O., K.Y., M.O. and Y.I. carried out experiments. M.N., C.A.M., K.I., J.K. and M.B. carried out analyses and provided general support. F.O. and S.K. wrote the paper.

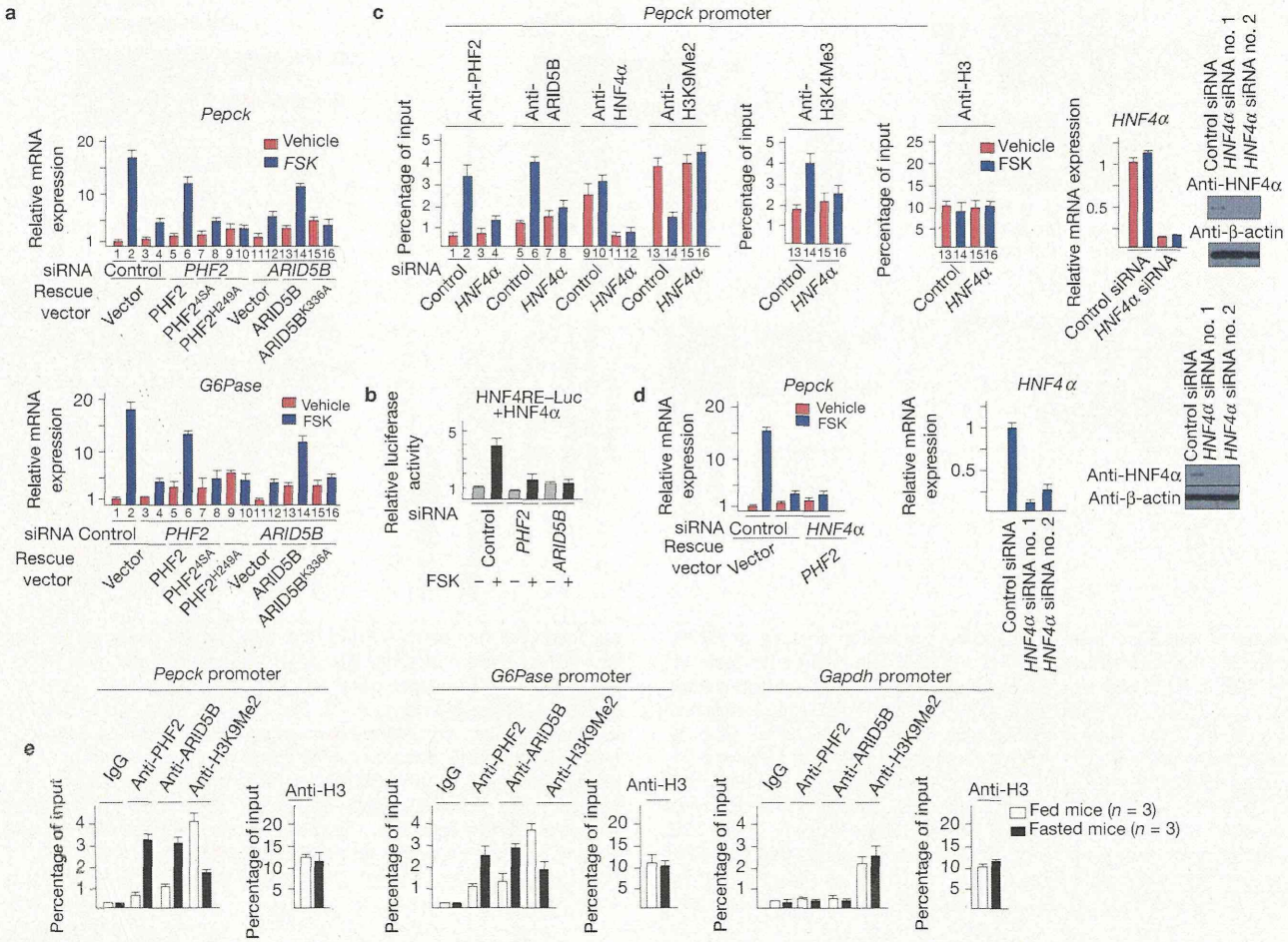

Figure 6 PHF2–ARID5B co-activates HNF4α in liver of fasted mice. (**a**) PHF2–ARID5B complex is indispensable for PKA-dependent gene induction of *Pepck* and *G6Pase*. Hepatocytes were transfected with the indicated siRNAs for 24 h, then incubated with the indicated compounds for 24 h, and quantatitive PCR with reverse transcription (RT–PCR) was carried out. Data are average ± s.d. ($n = 3$). (**b**) PHF2–ARID5B co-activates HNF4α in the presence of FSK in luciferase assays. 293F cells were transfected with the indicated plasmids in the presence or absence of FSK for 24 h. Data are average ± s.d. ($n = 3$). (**c**,**d**) Immortalized hepatocytes were transfected with HNF4α siRNA for 48 h, and ChIP assay (**c**) and quantitative RT–PCR for gene expression (**d**) were carried out. Knockdown efficiency was determined in the right panels of (**c**) and (**d**). Data are average ± s.d. ($n = 3$). (**e**) Livers from either fasted or fed mice ($n = 3$) were subjected to ChIP analyses using either anti-PHF2, anti-ARID5B, anti-H3K9Me2 or control IgG and anti-H3 antibodies. Fasting induces recruitment of PHF2–ARID5B and reduction of the H3K9Me2 mark in *Pepck* and *G6Pase* promoters, but not *Gapdh* promoter. Data shown are average ± s.d. of three independent experiments. Uncropped images of blots are shown in Supplementary Fig. S9.

COMPETING FINANCIAL INTERESTS
The authors declare no competing financial interests.

Published online at http://www.nature.com/naturecellbiology
Reprints and permissions information is available online at http://www.nature.com/reprints

1. Kouzarides, T. Chromatin modifications and their function. *Cell* **128,** 693–705 (2007).
2. Ruthenburg, A. J., Li, H., Patel, D. J. & Allis, C. D. Multivalent engagement of chromatin modifications by linked binding modules. *Nat. Rev. Mol. Cell Biol.* **8,** 983–994 (2007).
3. Iwase, S. *et al.* The X-linked mental retardation gene SMCX/JARID1C defines a family of histone H3 lysine 4 demethylases. *Cell* **128,** 1077–1088 (2007).
4. Klose, R. J., Kallin, E. M. & Zhang, Y. JmjC-domain-containing proteins and histone demethylation. *Nat. Rev. Genet.* **7,** 715–727 (2006).
5. Lee, M. G., Norman, J., Shilatifard, A. & Shiekhattar, R. Physical and functional association of a trimethyl H3K4 demethylase and Ring6a/MBLR, a polycomb-like protein. *Cell* **128,** 877–887 (2007).
6. Shi, Y. & Whetstine, J. R. Dynamic regulation of histone lysine methylation by demethylases. *Mol. Cell* **25,** 1–14 (2007).
7. Tsukada, Y. *et al.* Histone demethylation by a family of JmjC domain-containing proteins. *Nature* **439,** 811–816 (2006).
8. Christensen, J. *et al.* RBP2 belongs to a family of demethylases, specific for tri- and dimethylated lysine 4 on histone 3. *Cell* **128,** 1063–1076 (2007).
9. Klose, R. J. *et al.* The retinoblastoma binding protein RBP2 is an H3K4 demethylase. *Cell* **128,** 889–900 (2007).
10. Whetstine, J. R. *et al.* Reversal of histone lysine trimethylation by the JMJD2 family of histone demethylases. *Cell* **125,** 467–481 (2006).
11. Ohtake, F. *et al.* Dioxin receptor is a ligand-dependent E3 ubiquitin ligase. *Nature* **446,** 562–566 (2007).
12. Takada, I. *et al.* A histone lysine methyltransferase activated by non-canonical Wnt signalling suppresses PPAR-gamma transactivation. *Nat. Cell Biol.* **9,** 1273–1285 (2007).
13. Hasenpusch-Theil, K. *et al.* PHF2, a novel PHD finger gene located on human chromosome 9q22. *Mamm. Genome* **10,** 294–298 (1999).
14. Whitson, R. H., Huang, T. & Itakura, K. The novel Mrf-2 DNA-binding domain recognizes a five-base core sequence through major and minor-groove contacts. *Biochem. Biophys. Res. Commun.* **258,** 326–331 (1999).
15. Qi, H. H. *et al.* Histone H4K20/H3K9 demethylase PHF8 regulates zebrafish brain and craniofacial development. *Nature* **466,** 503–507 (2010).
16. Liu, W. *et al.* PHF8 mediates histone H4 lysine 20 demethylation events involved in cell cycle progression. *Nature* **466,** 508–512 (2010).
17. Tsukada, Y., Ishitani, T. & Nakayama, K. I. KDM7 is a dual demethylase for histone H3 Lys 9 and Lys 27 and functions in brain development. *Genes Dev.* **24,** 432–437 (2010).
18. Li, F. *et al.* Lid2 is required for coordinating H3K4 and H3K9 methylation of heterochromatin and euchromatin. *Cell* **135,** 272–283 (2008).

19. Lan, F. *et al. S. pombe* LSD1 homologs regulate heterochromatin propagation and euchromatic gene transcription. *Mol. Cell* **26,** 89–101 (2007).
20. Jiang, G. & Zhang, B. B. Glucagon and regulation of glucose metabolism. *Am. J. Physiol. Endocrinol. Metab.* **284,** E671–E678 (2003).
21. Lin, J., Handschin, C. & Spiegelman, B. M. Metabolic control through the PGC-1 family of transcription coactivators. *Cell Metab.* **1,** 361–370 (2005).
22. Mayr, B. & Montminy, M. Transcriptional regulation by the phosphorylation-dependent factor CREB. *Nat. Rev. Mol. Cell Biol.* **2,** 599–609 (2001).
23. Feige, J.N. & Auwerx, J. Transcriptional coregulators in the control of energy homeostasis. *Trends Cell Biol.* **17,** 292–301 (2007).
24. Goodwin, B. *et al.* A regulatory cascade of the nuclear receptors FXR, SHP-1, and LRH-1 represses bile acid biosynthesis. *Mol. Cell* **6,** 517–526 (2000).
25. Lu, T. T. *et al.* Molecular basis for feedback regulation of bile acid synthesis by nuclear receptors. *Mol. Cell* **6,** 507–515 (2000).
26. Koo, S. H. *et al.* The CREB coactivator TORC2 is a key regulator of fasting glucose metabolism. *Nature* **437,** 1109–1111 (2005).
27. Rhee, J. *et al.* Regulation of hepatic fasting response by PPARgamma coactivator-1α (PGC-1): requirement for hepatocyte nuclear factor 4α in gluconeogenesis. *Proc. Natl Acad. Sci. USA* **100,** 4012–4017 (2003).
28. Yoon, J. C. *et al.* Control of hepatic gluconeogenesis through the transcriptional coactivator PGC-1. *Nature* **413,** 131–138 (2001).
29. Fujiki, R. *et al.* GlcNAcylation of a histone methyltransferase in retinoic-acid-induced granulopoiesis. *Nature* **459,** 455–459 (2009).
30. Metzger, E. *et al.* LSD1 demethylates repressive histone marks to promote androgen-receptor-dependent transcription. *Nature* **437,** 436–439 (2005).
31. Rosenfeld, M. G., Lunyak, V. V. & Glass, C. K. Sensors and signals: a coactivator/corepressor/epigenetic code for integrating signal-dependent programs of transcriptional response. *Genes Dev.* **20,** 1405–1428 (2006).

DOI: 10.1038/ncb2228

METHODS

Plasmids. Full-length complementary DNAs of human PHF2, ARID5B (full length, β isoform), HNF-4α and FXR were inserted into pcDNA3 vectors (Invitrogen; ref. 11). Deletion mutants of PHF2 (amino acids 1–229 fused to amino acids 367–1103 for PHF2$^{\Delta jmjC}$) and ARID5B (amino acids 1–318 fused to amino acids 423–1188 for ARID5B$^{\Delta ARID}$) were amplified by PCR and cloned into pcDNA3 or pGEX4T-1 (Amersham). Point mutants of PHF2 (S1056A point mutation, or S797A, S899A, S954A and S1056A for PHF2^{4SA}) and PHF2 jmjC-domain point mutants (H249A, Y321A and H338A) and ARID5B were generated by site-directed mutagenesis. HNF4RE-tk–luciferase reporter plasmids were generated by insertion of the promoter region of consensus HNF4RE into a pGL3 luciferase plasmid[32]. FXRE-tk–luciferase reporter plasmids were generated by insertion of the promoter region of human SHP (−572 to −3) containing FXRE into a pGL3 luciferase plasmid. Other plasmids have been described previously[11,12,32,33].

Biochemical purification and separation of FXR- or PHF2-associated complexes. The hepatic tumour-derived *HepG2 cells* were incubated for 4 h with either FSK (1 μM) and/or H89 (1 μM), and the nuclear extracts were prepared as previously described. For purification of the FXR-associating complex, the nuclear extracts were bound to glutathione *S*-transferase (GST)–FXR(D/E)–His (amino acids 193–477) columns[11,12,33]. The bound complexes were eluted with reduced glutathione (15 mM) in elution buffer. Glycerol density gradients were carried out as previously described[11,12,33]. The complex fraction was further loaded onto a diethylaminoethyl column (Whatman), and eluted with different concentrations of NaCl (150 mM–1 M). The purified proteins were silver-stained, and identified by matrix-assisted laser desorption/ionization–time of flight mass spectrometry (Bruker)[11,12,33]. For purification of PHF2-associating complex, the nuclear extracts were loaded onto M2 anti-Flag agarose gel (Sigma, A2220, 069K6018). After washing with binding buffer, the bound proteins were eluted by incubation with 1.0 ml of the Flag peptide ($[EYKEEEK]_2$, 0.2 mg ml^{-1}) (Sigma).

***In vitro* and *in vivo* lysine demethylation assay.** The *in vitro* histone demethylation assays were carried out as previously described[7,10].

For preparation of demethylases from mammalian cells, 293F cells were transfected with Flag–PHF2 plasmid using Lipofectamine 2000 (Invitrogen). After 36 h, the cells were lysed with TNE (20 mM Tris at pH 7.8, 150 mM NaCl, 0.5 mM EDTA, 1% NP40). For phosphorylation of PHF2 *in vivo*, cells were treated with FSK (10^{-6} M) 2 h before harvest, and NaF/Na_2VO_3 added to TNE. Cell lysates were subjected to immunoprecipitation using anti-Flag antibody-conjugated beads (Sigma, A2220, 069K6018). Beads were washed three times with high-salt TNE (20 mM Tris at pH 7.8, 450 mM NaCl, 0.5 mM EDTA, 1% NP40), and then three times with EDTA-free TNE. For phosphorylation of PHF2 *in vitro*, beads were mixed with 20 μl PKA buffer (0.1 μg PKA (Upstate), 20 mM Tris at pH 7.5, 10 mM $MgCl_2$, 100 μM ATP and incubated for 1 h at 37 °C. Then, beads were washed three times with demethylase stock buffer (20 mM Tris at pH 7.5, 150 mM KCl, 10% glycerol). The prepared PHF2 protein was used immediately for the demethylation reaction. Alternatively, the purified proteins were eluted with Flag elution buffer (200 mg ml^{-1} Flag peptide, 20 mM Tris at pH 7.5, 450 mM KCl, 10% glycerol).

For preparation of recombinant proteins, recombinant Flag–PHF2 was purified using Bac-to-Bac baculovirus expression systems (Invitrogen) according to the manufacturer's instructions. The purified Flag–PHF2 complex was prepared as described in the section on biochemical purification.

For demethylase reaction, 2 μg of PHF2 protein or 0.2 μg of PHF2 complex was mixed with substrates (calf thymus histone (10 μg) (Sigma, H9250), purified mononucleosome (10 μg), Flag–ARID5B protein purified from 293F cells (2 μg) or dimethyl H3 (Lys 9) peptide 1–21 (0.2 μg) (Upstate 12–430)) in the reaction buffer (final volume 20 μl) (20 mM Tris-HCl at pH 7.5, 150 mM KCl, 50 μM $Fe(NH_4)_2(SO_4)_2$–$6H_2O$, 1 mM α-ketoglutarate, 1 mM ascorbate, 20 μM $ZnCl_2$). The mixtures were incubated at 37 °C for 12 h, terminated by boiling for 5 min in SDS sample buffer[7,10]. The histone modification or methylation of ARID5B was detected by specific antibodies (see the antibody section). The signal intensity of western blots was quantified using Scion Image.

For histone demethylase assay detecting formaldehyde release, purified PHF2 complex (0.2 μg) was incubated with native histones (10 μg) for 30 min according to the manufacturer's protocol using DetectXTM (LUMINOS, K010-F1).

For *in vivo* histone demethylation assay, cells were first lysed in TNE, and the pellet fraction was resuspended in TNE and sonicated for 20 s (Tomy SEIKO) to obtain the chromatin fraction[3,9,10,34].

Antibodies, immunoprecipitation and western blotting. Anti-PHF2 and anti-ARID5B polyclonal antibodies were raised against PHF2 peptides (5′-ERSVDVTDVTKQKDC-3′, 5′-CKPKPVRDEYEYVSD-3′, 5′-CAYKSDDSSDE-GSLH-3′) and ARID5B peptides (5′-CDTPQGRNSDHGEDE-3′, 5′-CTDQGSNSEK-VAEEA-3′, 5′-CEQTSKYPSRDMYRE-3′), respectively, by Operon Biotechnology. Anti-ARID5B K336Me2 antibody was raised using the dimethylated peptide (MKER(KMe2)TPIER: ARID5B K336Me2), and purified over a peptide affinity column (MBL). The antibodies that bound to the non-methylated peptide (MKERKTPIER) were removed using an affinity column. The specificity of the antibody toward K336Me2 over K336Me0, Me1 and Me3 peptides was determined in Supplementary Fig. S20 using enzyme-linked immunosorbent assays (MBL).

For immunoprecipitation, cells were treated with FSK (1 μM) or glucagon (200 nM) for 2 h and cells were lysed in TNE. Cell lysates were incubated with the indicated antibodies listed in Supplementary Table S1. A full list of antibodies and the dilutions used is given in Supplementary Table S1.

Cell culture, transfection and luciferase assays. Mouse immortalized hepatocytes, TLR2 cells, were obtained from RIKEN (cell no. RCB0750; ref. 35). The immortalized hepatocytes were cultured at 33 °C in DMEM containing 2% fetal bovine serum, 10 μg ml^{-1} transferrin, 1 μg ml^{-1} insulin and 10 ng ml^{-1} epidermal growth factor, using collagen-coated dishes. Other cell lines are cultured in DMEM supplemented with 10% fetal bovine serum. Cells were treated with glucagon (200 nM), FSK (1 μM), H89 (1 μM), CHX (1 μM), GW4064 (1 μM), dexametasone (10 nM) or 25-OH cholesterol (10 μg ml^{-1}) either for 24 h (luciferase assays), for 6 h (*in vivo* demethylation assays) or for 2 h (immunoprecipitation).

For luciferase assays, cells at 40–50% confluence were transfected with the indicated plasmids (0.25 μg reporter plasmids, 0.1 μg HNF4α, 0.1 μg FXR, 0.05 μg of PHF2) using Lipofectamine reagent (Gibco BRL). Luciferase activity was determined with the luciferase assay system (Promega) as previously described[11,12,32,33].

ChIP experiments. ChIP assays were carried out essentially as previously described[11,12,33]. Hepatocytes were treated with glucagon (200 nM), FSK (1 μM) and/or H89 (1 μM) for 4 h or as indicated. Then, cells were subjected to ChIP experiment as described[11]. The precipitated DNA fragments were amplified by quantitative PCR (qPCR; TAKARA). For qPCR with reverse transcription, the specific primer sets were designed and provided by TAKARA. The primer sets are shown in Supplementary Table S1.

Fasting responses in mice. All mice were maintained according to the protocol approved by the Animal Care and Use Committee of the University of Tokyo.

For ChIP assays[11], eight-week-old C57BL/6 male mice were either deprived of food or fed for 6 h. Livers were isolated, minced and fixed in PBS containing 1% formaldehyde at 4 °C overnight. The cells were washed in PBS twice, then sonicated in PBS containing 0.2 mM EDTA and 1% Triton X-100. The cell lysates were subjected to ChIP assays as previously described[11].

RNA isolation and qPCR. Messenger RNA was isolated as previously reported[33]. For qPCR with reverse transcription, the specific primer sets were designed and provided by TAKARA. The primer sequences are shown in Supplementary Table S1, and the amount was normalized using glyceraldehyde-3-phosphate dehydrogenase.

RNA interference experiments. The siRNAs as shown in Supplementary Table S1, together with siCONTROL non-targeting siRNA no. 2 (catalogue no. D-001210-02-20), were synthesized by and obtained from Dharmacon/Thermo, and were transfected using Lipofectamine 2000 reagent (Invitrogen) as previously described[11]. The two siRNAs used for each experiment, and the results of target sequence no. 1 (for PHF2, ARID5B and HNF4α) are shown.

Immunostaining. Immunostaining was carried out essentially as previously described[36]. 293F cells were transfected with PHF2 or its derivatives, and 12 h after the transfection the cells were treated with FSK for 6 h, then fixed and subjected to immunostaining[36]. Antibodies used are described in the antibody section.

***In vitro* and *in vivo* kinase assays.** Recombinant GST–PHF2 deletion mutants expressed in *Escherichia coli* (1 μg), or Flag–PHF2 and its derivatives (1 μg) immunoprecipitated from 293F cells using anti-Flag antibody and eluted by Flag peptide, were incubated with PKA (Upstate; 2 ng) in reaction buffer (20 mM Tris-HCl at pH 7.5, 10 mM $MgCl_2$, γ −^{32}P ATP) in the presence or absence of PKA inhibitor (10 μM H89) for 15 min at 30 °C.

For detection of phosphorylated proteins in cells, hepatocytes were treated with the indicated ligands for 2 h, then subjected to phospho-protein purification using a PhosphoProtein Purification Kit (QIAGEN; ref. 12). Alternatively, cell lysates were immunoprecipitated using anti-PHF2 or anti-Flag as indicated, then western

blotted using anti-phospho-PKA-substrate antibody (Cell Signaling Technology, 100G7E, 9624S). For statistical analysis, the signal intensity of western blots was quantified using Scion Image, and the average ± s.d. of four independent experiments was shown with Student's *t*-test.

DNA precipitation assays. DNA precipitation assays were carried out essentially as described[33,37]. Human *Pck1* promoter (−312 ~ 23) was amplified by PCR using biotinylated primers. Then, the biotinylated DNA was annealed and bound to avidin beads (Invitrogen). 293F cells were transfected with Flag-ARID5B, HA-PHF2 and their derivatives, and incubated with/without FSK for 2 h. Cell lysates were incubated with the DNA-bound avidin beads for 30 min in TNE buffer. The samples were subjected to western blotting[33,37].

32. Unno, A. *et al.* TRRAP as a hepatic coactivator of LXR and FXR function. *Biochem. Biophys. Res. Commun.* **327,** 933–938 (2005).
33. Ohtake, F. *et al.* Modulation of oestrogen receptor signalling by association with the activated dioxin receptor. *Nature* **423,** 545–550 (2003).
34. Yokoyama, A., Takezawa, S., Schule, R., Kitagawa, H. & Kato, S. Transrepressive function of TLX requires the histone demethylase LSD1. *Mol. Cell Biol.* **28,** 3995–4003 (2008).
35. Puigserver, P. *et al.* Insulin-regulated hepatic gluconeogenesis through FOXO1-PGC-1α interaction. *Nature* **423,** 550–555 (2003).
36. Okada, M. *et al.* Switching of chromatin-remodelling complexes for oestrogen receptor-alpha. *EMBO Rep.* **9,** 563–568 (2008).
37. Fujiki, R. *et al.* Ligand-induced transrepression by VDR through association of WSTF with acetylated histones. *EMBO J.* **24,** 3881–3894 (2005).

nature cell biology

SUPPLEMENTARY INFORMATION

DOI: 10.1038/ncb2228

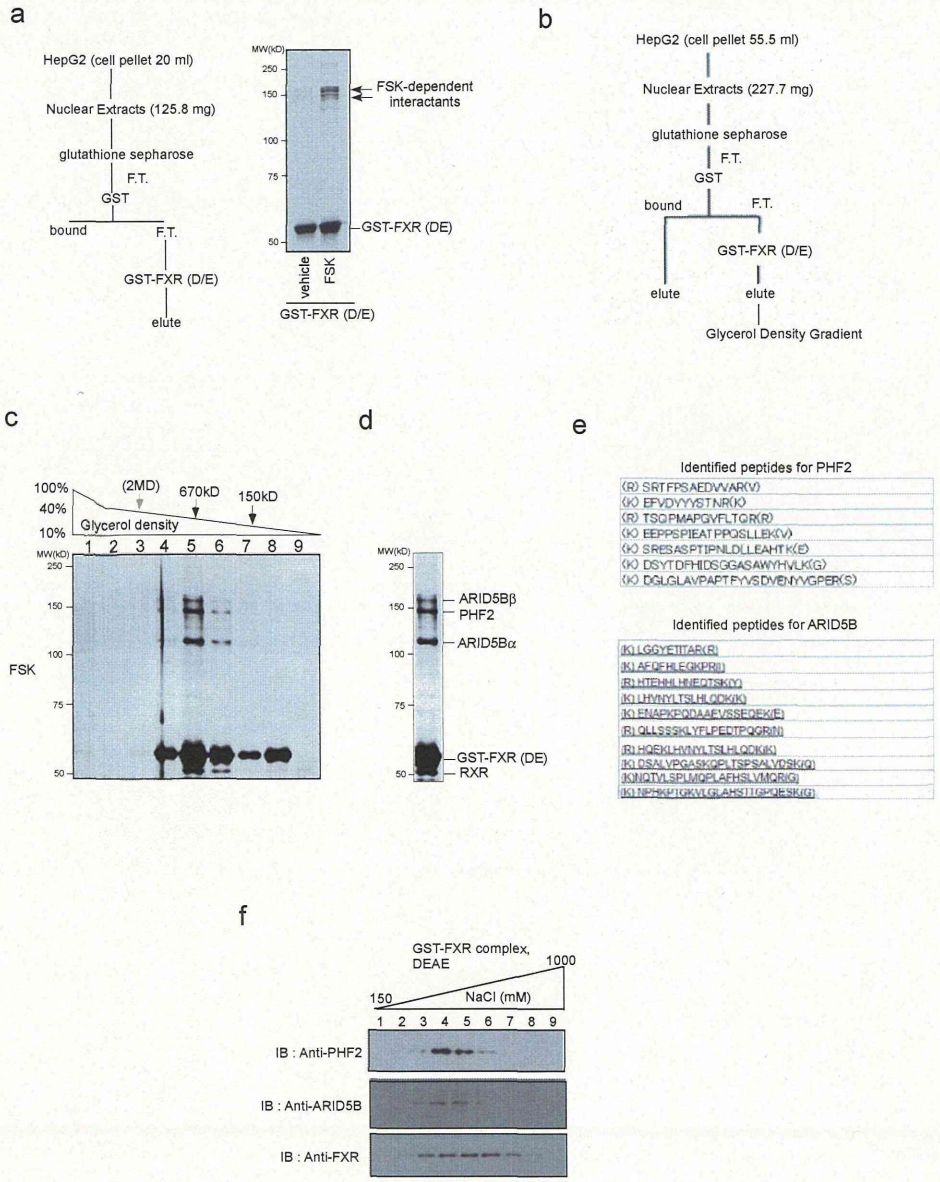

Figure S1 Purification of PHF2/ARID5B complex. **a,** Purification of a signal-dependent GST-FXR-associated proteins from HepG2 cells. Nuclear extracts from FSK-treated HepG2 cells were loaded on GST-FXR-bound glutathione sepharose beads. The bound proteins were analyzed by silver staining. **b,** The scheme for the purification of nuclear receptor-associating complexes. The experimental details were supplied in the supplemental methods. **c,** Purification of a GST-FXR-associated complex from HepG2 cells. Nuclear extracts from FSK-treated HepG2 cells were loaded on GST-FXR-bound glutathione sepharose beads. The eluted complexes were separated by glycerol density gradients as indicated. **d, e,** The isolated complexes were silver stained, and each protein was identified by MALDI-TOF/MS and fingerprinting. **f,** PHF2 and ARID5B form a complex with GST-FXR. The purified GST-FXR-associating complex in (c) was further separated by DEAE column with different NaCl concentrations. The elutants were subjected to Western blotting.

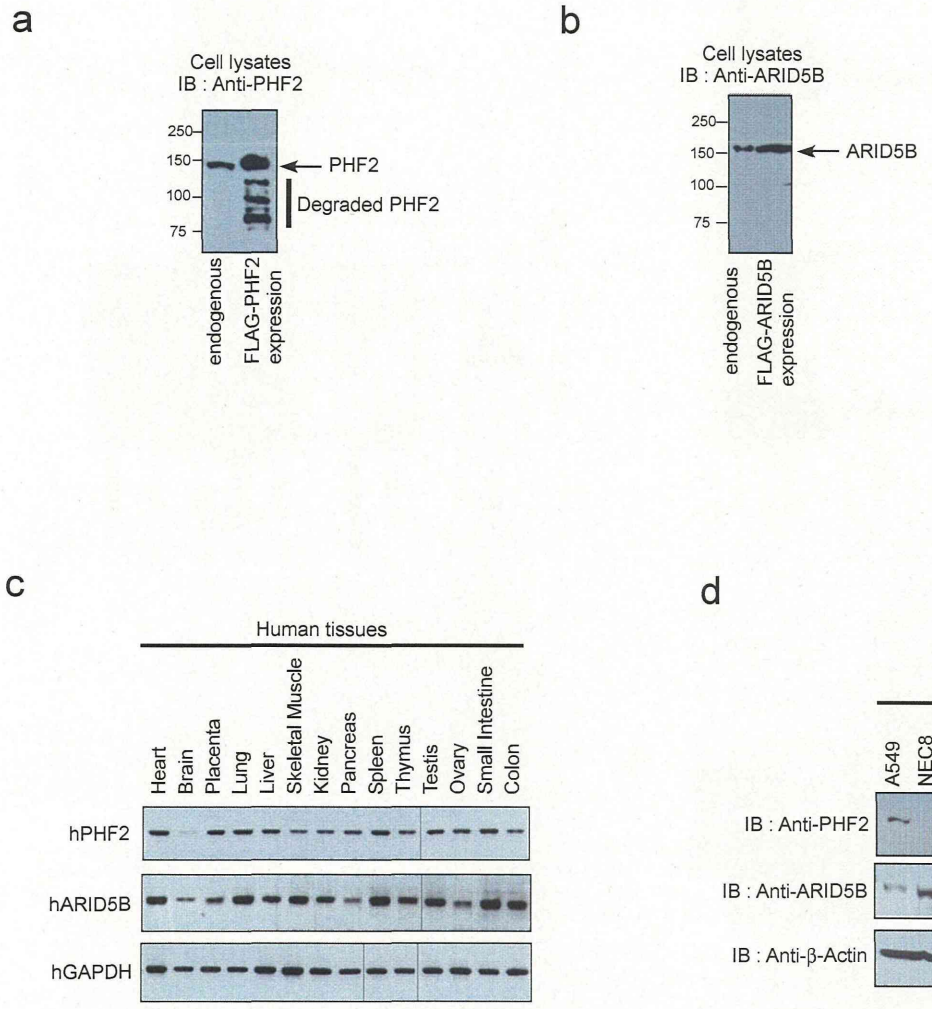

Figure S2 The expression profiles of PHF2 and ARID5B. **a, b,** Specificity confirmation of the newly raised antibodies. Normal 293F cell lysates or lysates transfected with the indicated expression vectors were subjected to Western blotting. This confirmed that these anti-PHF2 (a) and anti-ARID5B (b) antibodies detect endogenous proteins with high specificity. **c**, The mRNA expression profiles of human PHF2 and ARID5B. The mRNA levels of PHF2 and ARID5B were determined by semi-quantitative PCR using cDNAs from human tissues (Clontech, human cDNA panel, #636742 and #636743). **d**, Protein expression of PHF2 and ARID5B in various human cell lines. Total cell lysates were prepared from the indicated human cell lines. Equal amounts of proteins were subjected to Western blotting with the indicated antibodies.

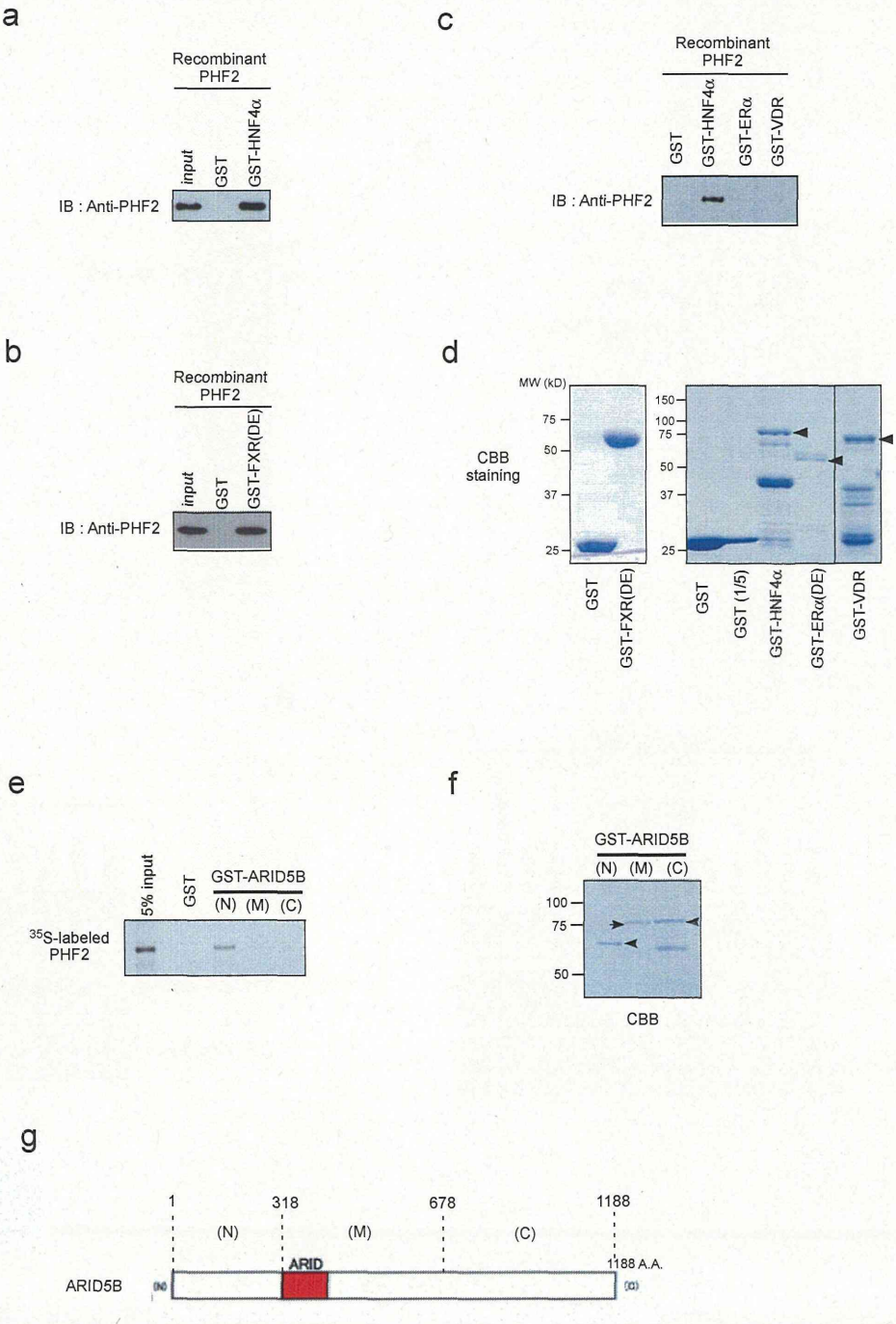

Figure S3 Direct association of PHF2/ARID5B with HNF4α and FXR. **a-d**, GST pull-down assay with recombinant PHF2 protein and GST-tagged FXR(DE), HNF4α, ERα (DEF), or VDR. Bound protein was detected with anti-PHF2 antibody. **e-g**, GST pull-down assay with ^{35}S-labeled PHF2 and GST-ARID5B mutants. GST-ARID5B mutants, described in (g), were incubated with *in vitro*-translated PHF2. Bound proteins were detected by autoradiography.